Two New Neutrophil Subsets Define a Discriminating Sepsis Signature

Aïda Meghraoui-Kheddar, Benjamin Chousterman, Noëlline Guillou, Sierra Barone, Samuel Granjeaud, Helene Vallet, Aurélien Corneau, Karim Guessous, Charles de Roquetaillade, Alexandre Boissonnas, et al.

Two new neutrophil subsets define a discriminating sepsis signature

Aïda Meghraoui-Kheddar[1]*, Benjamin G. Chousterman [2,3], Noëlline Guillou[1], Sierra M. Barone[4], Samuel Granjeaud[5], Helene Vallet[1,6], Aurélien Corneau[7], Karim Guessous[2], Charles de Roquetaillade [2,3] Alexandre Boissonnas[1], Jonathan M. Irish[4, 8], Christophe Combadière[1]*

Affiliations :

[1] Sorbonne Université, Inserm, CNRS, Centre d'Immunologie et des Maladies Infectieuses, Cimi-Paris, F-75013, Paris, France.
[2] AP-HP, CHU Lariboisière, Department of Anesthesia and Critical Care, DMU Parabol, FHU Promice, Paris, France
[3] Université de Paris, Inserm U942 MASCOT, Paris, France
[4] Department of Cell and Developmental Biology, Vanderbilt University, Nashville, TN, USA
[5] CRCM, Inserm, U1068; Paoli-Calmettes Institute; Aix-Marseille University, UM 105; CNRS, UMR7258, Marseille, France.
[6] Acute geriatric unit, Saint Antoine Hospital, Assistance-Publique Hôpitaux de Paris, Paris, France.
[7] Sorbonne Université, UMS037, PASS, CyPS, Paris, France.
[8] Department of Pathology, Microbiology and Immunology, Vanderbilt University Medical Center, Nashville, TN, USA

* Corresponding author information :
Christophe Combadière, PhD,
Centre d'Immunologie et des Maladies Infectieuses (Cimi-Paris),
91 Boulevard de l'Hôpital, Faculté de Médecine Sorbonne université, site Pitié, 75013 Paris, France,
Tel: +33 140 779 897
e-mail: christophe.combadiere@upmc.fr
Aïda Meghraoui-Kheddar, PhD, PharmD,
Institut de Pharmacologie Moléculaire et Cellulaire, IPMC UMR7275,
660 route de Lucioles, Sophia Antipolis, 06560 Valbonne, France,
Tel: +33 4 93957781
e-mail: aida.meghraoui-kheddar@inserm.fr

Authorship contributions:

AMK, BGC, AB and CC designed the study. AMK and NG performed experimental work. BGC, KG, CdR and HV provided clinical samples, pathological diagnosis and patient clinical data. AMK compiled patient data. AMK and AC run samples in the mass cytometer. AMK, SMB, SG and JMI performed data analysis. AMK, JMI and CC developed the figures, and wrote the manuscript. CC provided financial support. All authors contributed in reviewing the manuscript.

Running head: Sepsis neutrophil signature for patients' diagnosis

Subject Category: 7.19 Neutrophils

Text word count: 4344

At a Glance Commentary:

There is an unmet need for specific and rapid diagnostic tests for sepsis, which would discriminate sepsis patients from patients with aseptic inflammation. This work represents the first comprehensive evaluation of whole blood circulating immune cells in septic patients using CyTOF high-dimensional technology coupled with computational analysis. It allowed the identification of two novel sepsis-specific neutrophil subsets: CD10-CD64+PD-L1+ and CD10-CD64+CD16low/-CD123+ immature neutrophils. This early sepsis immune cell signature was validated computationally and biologically in an independent cohort and could be used for sepsis diagnosis.

Abstract:

Rationale: Sepsis is the leading cause of death in adult intensive care units. At present, sepsis diagnosis relies on non-specific clinical features. It could transform clinical care to have immune cell biomarkers that could predict sepsis diagnosis and guide treatment. For decades, neutrophil phenotypes have been studied in sepsis, but a diagnostic cell subset has yet to be identified.

Objectives: To identify an early specific immune signature of sepsis severity that does not overlap with other inflammatory biomarkers, and that distinguishes patients with sepsis from those with non-infectious inflammatory syndrome.

Methods: Mass cytometry combined with computational high-dimensional data analysis were used to measure 42 markers on whole blood immune cells from sepsis patients and controls, and automatically and comprehensively characterize circulating immune cells, which enables identification of novel, disease-specific cellular signatures.

Measurements and Main Results: Unsupervised analysis of high-dimensional mass cytometry data characterized previously unappreciated heterogeneity within the $CD64^{+}$ immature neutrophils and revealed two new subsets distinguished by CD123 and PD-L1 expression. These immature neutrophils exhibited diminished activation and phagocytosis functions. The proportion of CD123-expressing neutrophils correlated with clinical severity.

Conclusions: This study showed that these two new neutrophil subsets were specific to sepsis and detectable by routine flow cytometry using seven markers. The demonstration here that a simple blood test distinguishes sepsis from other inflammatory conditions represents a key biological milestone that can be immediately translated into improvements in patient care.

Abstract word count: 232

Key words: Sepsis, neutrophils, diagnosis, PD-L1, CD123

Introduction

Sepsis is the leading cause of death in the intensive care unit (ICU) (1-3). Diagnosis of patients relies on clinical data rather than a robust biomarker that distinguishes sepsis from sterile inflammation and predict its clinical outcome and prognosis can be evaluated by several scores including Simplified Acute Physiology Score II (SAPS II) and Sequential Organ Failure Assessment (SOFA) Score. SOFA and SAPS-II are indicators of severity, show poor performance regarding sepsis diagnostic and were consistently shown to be non-specific of sepsis (1, 4-7). It is estimated that the survival rate decreases by roughly 10% every hour that appropriate antimicrobial medication is delayed, emphasizing the urgent need for early diagnosis techniques (8, 9). A comprehensive systems immunology approach using mass cytometry is well-suited to characterize the diversity of disease-specific cellular states (10). Neutrophils are a primary immune cellular barrier against pathogens, but they may be a double-edged sword in sepsis having a role in both inflammation and immunosuppression (11-15). We hypothesized that phenotype of circulating neutrophils might provide crucial early insight into immune features that drive sepsis and distinguish this disease from non-infectious inflammatory syndrome.

For the systems immunology approach here, it was critical to track features that had been identified as important in sepsis biology, but which individually had not the resolving power to specifically distinguish sepsis. Neutrophils expressing the high-affinity immunoglobulin-Fc receptor I (CD64) were described in numerous clinical studies over the last two decades (16). CD64 is normally expressed on monocytes, but its expression on circulating neutrophils could be due to its upregulation during inflammation (17), or to released immature granulocytes from the bone marrow, especially when it is associated with decreased expression of neutral endopeptidase (CD10) and low-affinity immuno-globulin-Fc fragment III (CD16) (13, 14, 18) (Supp.Tab.1) (19). Previous studies identified also the interleukin (IL)-3 as an orchestrator of emergency myelopoiesis during sepsis and showed its association with hospital mortality (20, 21). In

parallel, programmed death ligand-1 (PD-L1) expressed on monocytes was also described as a mortality-predictor in sepsis patients (22, 23).

A systems-level view is likely needed to identify cellular features that specifically distinguish sepsis infection-induced immune phenotypes from those triggered by aseptic inflammatory signals. To identify such early sepsis-specific cellular biomarkers, we developed a multi-parametric immune profiling strategy (Fig.1). Cytometry by Time-Of-Flight (CyTOF) instrument was used to measure 42 markers on whole blood immune cells from sepsis patients and controls (Fig.1A) (24). A computational analysis approach was used to comprehensively characterize circulating immune cells and identify disease-specific cellular signatures (25, 26). This approach consisted in a "discovery strategy" (Fig.1B) and a computational "validation strategy" (Fig.1C) based on two complementary set of algorithms. We identified two unreported early and sepsis-specific neutrophil subsets. A conventional "expert driven strategy" using a limited set of markers confirmed that these two sepsis-specific neutrophil subsets were associated with sepsis (Fig.1D). This result was confirmed using an independent cohort of patients and conventional flow cytometry (Fig.1E).

Methods

Study design

This observational study was approved by the Comité de Protection des Personne Paris VII ethic committee (CPP IDF VII A000142-53). Two cohorts were used in this study (Supp.Tab.2). Seventeen sepsis (S) patients and twelve patients undergoing cardiac surgery considered as non-infected inflammatory controls (NIC) were included in the discovery cohort of the study (Supp.Tab.2). The validation cohort was composed of twenty-four sepsis patients and eighteen non-infected patients with

106 confoundable symptoms of sepsis (NIP) (Supp.Tab.2). Blood samples were drawn in heparin-coated
107 tubes, collected at the first- and seventh-day post admission of antibiotic treated sepsis patients or post-
108 surgery for NIC patients of the discovery cohort, and at the first-day post admission of the validation
109 cohort patients. In addition, blood samples of eleven age and gender matched healthy donors (HD)
110 were obtained from the French blood donation center. Five bone marrow (BM) biopsies from
111 orthopedic surgery patients were also included in this study.

112 *Mass cytometry analysis*

113 Whole blood samples were stained using a 42-dimensional mass cytometry panel (Supp.Tab.3). A
114 multi-step staining protocol was set up and is detailed in the supplementary methods section. Once the
115 collection of samples was completed, stained cells were thawed then measured on a CyTOF Helios
116 instrument. Acquired data were normalized with a MATLAB-based software (27) and analyzed using
117 the Cytobank platform (28).

118 *Computational data analysis*

119 To identify immune subsets and visualize all cells in a 2D map where position represents local phenotypic
120 similarity, we used two different dimensionality reduction tools depending on the strategy: the viSNE
121 implementation of t-SNE (29) and the UMAP (30). Cells were also grouped in phenotypically
122 homogenous clusters using either SPADE (31) or FlowSOM (32, 33). To phenotypically characterize
123 these clusters, Marker Enrichment Modeling (MEM) (34, 35) was used. The analysis process of each
124 strategy is detailed in the supplementary methods section.

125 *Flow cytometry validation panel*

To validate the sepsis-specific neutrophils signature a seven markers panel (Supp.Tab.4) was designed for conventional florescent flow cytometry. The sepsis samples were analyzed in a blind cytometry testing, along with the non-infected patients. The staining protocol is detailed in the supplementary methods section.

Activation and phagocytosis assay

To address neutrophils activation and phagocytic capacities we used pHrodo-labeled BioParticles and coated with *Staphylococcus aureus* (*S. aureus*) or Zymosan antigens (Invitrogen). The staining protocol is detailed in the supplementary methods section.

Statistical information

Numerical data are given as median and inter-quartile range (25th - 75th percentile) with the exception of Fig.7 data that are given as mean±SD. Nonparametric two-tailed Mann-Whitney test with a significance threshold of alpha (α=0.05) was used to compare cellular abundances of cell subsets between two groups of patients and MFI ratios. Nonparametric two-tailed Wilcoxon signed-rank test with a significance threshold of alpha (α=0.05) was used to compare cellular abundances of cell subsets from patients at day-1 and day-7. Relationship between two data sets was assessed using Spearman's rank correlation coefficient (r) and test with a significance threshold of alpha (α=0.05), and linear regression line was drawn on the corresponding plot. Statistical tests were performed using GraphPad7 software (GraphPad Software, San Diego, CA), as well as receiver operator characteristic (ROC) analyses.

Results

Mass cytometry and computational analysis revealed a sepsis-specific neutrophil signature

We designed a longitudinal observational study with 40 individuals to explore the evolution of circulating immune cell phenotypes of S patients (n=17), NIC patients (n=12) at day 1 and 7 (Supp.Tab.2) and HD (n=11) in addition to BM biopsies (n=5) (Fig.1A). Whole blood immunostaining was performed with a 42-parameter mass cytometry panel designed to give a comprehensive evaluation of circulating leukocytes (Fig.1A, Supp.Tab.3). We identified circulating immune cell populations. Using viSNE tool, neutrophils were gated, and other circulating immune cells were independently analyzed.

The neutrophils were analyzed with a "discovery strategy" using viSNE and SPADE tools (Fig.1B). viSNE is an unsupervised algorithm that reduces feature dimensions and allows cells visualization in a two-dimensional map. SPADE is an unsupervised algorithm aiming to group cells into nodes that could be displayed on the viSNE map. This strategy allowed to define an imprint for each sample group (Fig.2A). On the resulting map, neutrophils of S and NIC day-1 patients and neutrophils of HD were arranged in three different areas (Fig.2A). These S neutrophils were clustered in specific nodes that were absent from NIC and HD (Supp.Fig.1, 2). Some of these S specific nodes were shared with BM, suggesting the occurrence of myelocytosis for S patients (Supp.Fig.1, 2). Most cells from day-7 samples were phenotypically similar to samples from HD (Fig.2A, Supp.Fig.1, 2). CD16, CD10 and CD64 markers split neutrophils signature into two positive and negative subpopulations for each marker (Supp.Fig.1). To characterize all the nodes, their abundance in each sample and their average expression of each marker were extracted and used to generate two heatmaps (Supp.Fig.3, 4). Hierarchical clustering was used to arrange rows (nodes) and columns (samples) of the frequency heatmap (Supp.Fig.3) and columns (markers) of the phenotype heatmap (Supp.Fig.4). In this unsupervised three arms analysis (nodes, samples and markers), the resulting dendrograms led to the identification of 3 main samples clusters (columns) as shown in Fig2B (Supp.Fig.3 before tree cut). Most of the samples were clustered

according to patient groups. S day-1 (pink) and BM (orange) samples were clustered together. S day-7 samples were split in two sample clusters, with half of them clustering with HD samples (Fig2B, Supp.Fig.3) suggesting the acquisition of a "healthy" neutrophil phenotype profile (Fig2A). In addition, this unsupervised strategy allowed the precise delimitation of four groups of cell nodes (Fig.2D): (1) HD-abundant nodes representing neutrophils with $CD16^{high}CD10^{med}CD64^{-}$ phenotype, (2) NIC and S day-7 common nodes harboring $CD16^{+}CD10^{med}CD64^{-}$ phenotype, (3) day-1 NIC and S common nodes defined as $CD16^{low}CD10^{-}CD64^{low}$, and (4) S day-1 and BM nodes with $CD10^{-}CD64^{+}$ phenotype. Node group (4) represents cells that are highly abundant in sepsis samples at day-1 when compared to other patient groups (Supp.Fig.5A). The statistical analyses of these nodes are presented in Supp.Fig.5B. Among the nodes that statistically discriminate S and NIC at day-1 (Supp.Fig.5B), a specific phenotypic characteristic was observed: three nodes expressed CD123 and four other nodes expressed PD-L1 (Supp.Fig.5A, Fig.2C, D). On the basis of phenotypic homogeneity meta-clusters were generated to group nodes that share similar expression of these two markers and represent two neutrophil subsets specific to S at day-1 and observed to be lacking in NIC neutrophils (Fig.2E). The first subset (in red) was composed of $CD10^{-}CD64^{+}CD16^{+}PD\text{-}L1^{+}$ neutrophils (S median proportion: 18.08 (6.69-48.33) %, NIC median proportion: 0.81 (0.53-3.01) %, *p=0.0002*) and the second one (in blue) identified as $CD10^{-}CD64^{+}CD16^{low}CD123^{+}$ immature neutrophils (S median proportion: 10.06 (1.12-39.35) %, NIC median proportion: 0.04 (0.02-0.42) %, *p<0.0001*) (Fig.2E). We also recapitulated previously described results (13, 14, 18) regarding the sepsis related increase of circulating immature $CD10^{-}CD64^{+}$ neutrophils when compared to NIC at day-1 (S median proportion: 11.03 (1.41-40.39) %, NIC median proportion: 0.62 (0.12-1.46) %, *p=0.001*) and we confirmed their phenotypic similarities with a third of BM neutrophils (BM median proportion: 37.39 (17.90-46.48) %) (Fig.2E). Also, we noticed that all HD specific-nodes were absent in S patient day-1 samples (Fig.2B, D).

With this strategy, two novel neutrophil subsets were identified, including $CD123^+$ cells (red) and $PD\text{-}L1^+$ cells (blue), and the absence of HD neutrophil phenotypes at an early stage of sepsis.

A computational validation strategy confirmed sepsis day-1 specific neutrophil subsets

To test whether the previously identified neutrophil subsets were sepsis-specific and robust, an independent unsupervised data analysis strategy was applied on the same data files used in the discovery strategy (Fig.1B, C). This "validation strategy" was based on UMAP and FlowSOM algorithms. UMAP is an unsupervised dimensional reduction algorithm (Supp.Fig.6A) and FlowSOM is an unsupervised clustering algorithm. This strategy allowed the identification of 50 neutrophil clusters and the complete linkage hierarchical clustering of their relative cell abundance arranged again the samples according to patient groups (Supp.Fig.6B). Two main cell cluster groups (pink gates) appeared to be more abundant in sepsis samples (Supp.Fig.6B, C) and almost all HD associated-clusters (purple gate) were absent in sepsis patient day-1 samples.

To phenotypically characterize the pink gate clusters, MEM phenotype annotation tool was used. The MEM label of each cluster is an objective description of what makes that subset distinct from all the other clusters. Among these clusters, three cell meta-clusters were identified, one with $CD10^-CD64^+$ immature cells (pink clusters), and two meta-clusters phenotypically identical to the "discovery strategy" sepsis-specific neutrophils nodes (Supp.Fig.6D, Fig.3A). Red clusters contained $CD10^-CD64^+PD\text{-}L1^+$ neutrophils with a median cell proportion of 5.50 (1.15-38.03) % for S day-1 samples and 0.09 (0.02-0.33) % for NIC day-1 samples ($p<0.0001$) (Fig.3B). Blue clusters gathered $CD10^-CD64^+CD16^{low/-}$ $CD123^+$ immature neutrophils with median cell proportions of 2.43 (0.98-6.32) % and 0.04 (0.03-0.28) % for S day-1 and NIC day-1 samples respectively ($p=0.0006$) (Fig.3B). We also visually noted that red clusters ($PD\text{-}L1^+$ cells) and blue clusters ($CD123^+$ cells) from the "validation strategy" are co-localized

with red nodes (PD-L1$^+$ cells) and blue nodes (CD123$^+$ cells), respectively, from the "discovery strategy", when back mapped onto the t-SNE1-2/t-SNE2-2 axes (Fig.3C).

Expert gating strategy based on a limited set of markers validated the sepsis day-1 neutrophil signature that correlates with SAPSII and SOFA scores

After cell subsets were identified by automatic and high-dimensional analysis strategies, we determined whether the identified neutrophil signature could be found using conventional analysis applicable by experts. The use of such gating strategy would make it easier to transpose it to clinical use.

A bi-parametric gating strategy on a limited set of markers allowed the identification of neutrophils expressing CD123 and PD-L1 (Fig.4A). When CD123$^+$ and PD-L1$^+$ sepsis-specific neutrophils were mapped back onto both t-SNE1-2/t-SNE2-2 axes and UMAP1/UMAP2 axes, they located in the same regions as the cells identified by the two previous computational strategies meaning that they share the same phenotype (Fig.4A). This expert gating strategy applied on the current dataset, allowed the selection of PD-L1 expressing neutrophils that were significantly more abundant in blood of S day-1 patients (9.25 (3.61-36.97) %) when compared to NIC day-1 patients (0.12 (0.07- 0.60) %, $p<0.0001$) or HD (0.01 (0.00-0.03) %, $p<0.001$) (Fig.4B). Similarly, expert gating allowed the selection of S-specific neutrophils (2.47 (0.44-17.42) %) that were consistent with CD123$^+$ red subsets cells phenotype and that were almost absent from NIC (0.04 (0.07-0.87) %, $p<0.0001$) or HD (0.04 (0.02-0.10) %, $p<0.0001$) (Fig.4B).

Although the proportion of CD10-CD64+CD16-CD123+ neutrophils could distinguish S and NIC samples at day 1, we observed a large variability between patients. Interestingly, we noticed that patients with the highest CD123+ neutrophil subset proportion (> 20%) tended to be more severe (requirement for mechanical ventilation and catecholamine support). Later correlation with severity scores confirmed this observation. The proportion of CD123$^+$ sepsis-specific, assessed by the simple gating strategy on mass

cytometry data, positively correlated with Simplified Acute Physiology Score II (SAPS II) (Spearman r=0.62, p=0.0192) and Sequential Organ Failure Assessment (SOFA) score (Spearman r=0.55, p=0.0437) (Fig.4C). However, the proportion of CD123+ neutrophil was not influenced by sepsis endotype. The proportions of PD-L1 neutrophil subset did not correlate with severity scores nor sepsis endotypes. ROC analysis of these CD123+ neutrophils abundance was carried out to determine the optimal threshold separating sepsis patients from non-infected patients. A cut-off point of 0.38% of the CD123+ neutrophil subset abundance was able to identify sepsis patients with a specificity of 91.67% and sensitivity of 81.25% and display an area under the ROC curve (AUROC) of 0.91 (Fig.4D). When combining the abundance of the CD123+ and PD-L1+ neutrophil subsets, the cut-off point changed to 0.93% and lowered both the sensitivity, to 75%, and the specificity, to 83.33%. (Fig.4E). Whereas a clinical SOFA score >2 was discriminating with a good sensitivity (94.12%) but with a poor specificity (45.45%) and a worst AUROC of 0.79 (Fig.4F). In addition, the AUROC of SAPS-II score was also lower (AUROC=0.82) with a sensitivity of 88.24% and a poor specificity of 45.45% (Fig.4G).

Thus, a simple gating strategy assessing only 7 key markers identified successfully CD123+ and PD-L1+ sepsis-specific neutrophils and indicated that CD123+ neutrophils may be a marker of sepsis severity with a better discriminating efficiency when compared to clinical scores.

Mass cytometry and unsupervised analysis identified classical sepsis immune hallmarks

Using two complementary computational strategies, we identified a sepsis-specific signature on the neutrophil cells. We asked whether a signature in the non-neutrophil cells could reinforce the $CD123^+$ and $PD\text{-}L1^+$ neutrophil subsets as sepsis biomarker candidates. The non-neutrophils circulating immune cells were computationally analyzed using t-SNE and SPADE algorithms. A heatmap was generated to characterize nodes phenotype and to delimitate the main circulating non-neutrophil immune cell

populations, according to complete linkage hierarchical clustering (Supp.Fig.7A). These populations were then color coded and backgated on the t-SNE map (Supp.Fig.7B). Classical hallmarks of sepsis were identified, including lymphopenia, monocytopenia and a persistent lower level of monocytes HLA-DR in S patients when compared to HD group ($p<0.0001$, $p=0.0426$ and $p<0.0001$ respectively, Fig.5A). In parallel, we observed an elevated number of circulating neutrophils *(*$p=0.0039$), and consistent with that, a higher neutrophil to lymphocyte ratio ($p<0.0001$) in S vs. HD (Fig.5B). These trends were not exclusive to S, but were also observed in NIC group when compared to HD group ($p=0.0003$, $p<0.0001$, $p=0.0034$, $p<0.0001$, for lymphocytes and neutrophils counts, monocytes HLA-DR expression level and neutrophils/lymphocytes ratio, respectively). No significant difference was observed between S and NIC group at day-1 within these main immune cell populations (Supp.Tab.2).

To identify an early sepsis-specific signature within these immune populations, we compared the abundance of the identified cell nodes of these immune populations between HD, NIC and S samples at day-1. The abundance of 22 nodes was found selectively regulated in S at day-1 when compared to both NIC and HD and 25 nodes differentiated S only from NIC at day-1 (Supp.Fig.7C, D). It included notably 15 nodes identifying classical monocytes with high expression of HLD-DR, 3 nodes of $CD4^+$ T lymphocytes and $CD8^+$ T lymphocytes expressing CCR2 and CCR6, all were highly reduced in S patients, one node of B lymphocytes with a low expression of B cells pan markers (HLD-DR, CXCR5, CD19 and CCR6) and one node identified monocyte-derived DC (Fig.5C). Among the nodes that were massively reduced in both S and NIC sample, 15 nodes out of 55 represent Basophils and Eosinophils subsets (Fig.5D); the others being scattered among other cell populations.

Taken globally, the analysis of circulating non-neutrophil cells with a computational strategy allowed us to resume sepsis hallmarks and identify the differences of several circulating immune subsets abundance.

CD123+ and PD-L1+ sepsis-specific neutrophils are detectable by conventional cytometry and discriminate infected and non-infected patients

We identified two neutrophil subsets using 40 individuals and 42-marker mass cytometer and computational analysis. These subsets might be detectable by conventional cytometry approach that is used in routine in the clinic. To evaluate the efficiency and specificity of $CD123^+$ and $PD\text{-}L1^+$ neutrophil subsets to discriminate sepsis patients from non-infected ones, we set up a fluorescent 7-marker flow cytometry panel (Supp.Tab.4). We monitored an independent validation cohort composed of non-infected patients (n=18) and sepsis patients (n=24).

With the overlay of full minus-two (FMT) stained control and the full panel stained tubes of three representative patients of several expression levels of CD10, CD123 and PDL1, we appreciated the increase of $CD123^+$ and $PD\text{-}L1^+$ sepsis-specific neutrophil subsets with the decrease of CD10 expression by neutrophils ($CD14^-CRTH2^-CD15^+$ cells) (Fig.6A). ROC analysis was performed using $CD123^+$ and $PD\text{-}L1^+$ neutrophil subsets abundances, measured by conventional flow cytometry on an independent validation cohort of sepsis and non-infected patients. A cut-off point of 0.35% of the $CD123^+$ neutrophil subset abundance was able to rule out sepsis patients with a specificity of 94.44% and sensitivity of 87.5% and an AUROC of 0.95 (Fig.6B). When combining the abundance of the $CD123^+$ and $PD\text{-}L1^+$ neutrophil subsets, the cut-off point changed to 0.60% with no effect on the sensitivity nor on the specificity (Fig.6C). Whereas, a clinical SOFA score >2 was discriminating with a good sensitivity (91.30%) but with a poor specificity (18.18%) and a worst AUROC of 0.61 (Fig.6D). In addition, the AUROC of SAPS-II score was also lower (AUROC=0.69) with a sensitivity of 91.67% and a poor specificity of 25.00% (Fig.6E). These results indicated that conventional flow cytometry recapitulates the results obtained by mass cytometry and confirmed that the identified neutrophil subsets could be a marker of sepsis severity with

303 a better efficiency than clinical scores and reliably quantified by routinely performed clinical flow
304 cytometric profiling

305 In addition, we evaluated if the CD123+ neutrophil subset was only abundant in patients with the highest
306 severity scores. We used the data generated in both the discovery (Fig.4) and the validation cohorts (Fig.6)
307 and divided the cohorts by quartile of severity according to SOFA and SAPS II scores (Supp.Fig.8A, B).
308 While sepsis and non-infected patients overlap greatly their severity scores, the proportion of CD123+
309 neutrophils subset distinguishes efficiently sepsis and control groups in both discovery (Supp.Fig.8A) and
310 validation cohorts (Supp.Fig.8B).

311 *Immature sepsis neutrophils exhibit an impaired microbial specific activation and phagocytosis*

312 To address sepsis-associated neutrophils activation and phagocytic capacities, whole blood of each tested
313 individual was incubated with *Staphylococcus aureus* (*S. aureus*) or Zymosan coated bio-particles labelled
314 with pHrodo, a pH-sensitive fluorochrome (36), in order to identify immature neutrophils bio-particles
315 uptake capacity and activation.

316 All immature circulating neutrophils (CD64+CD10^{-}) were able to phagocyte *Staphylococcus aureus* (*S.*
317 *aureus*) beads independently from their group (HD, S-D1, BM). However, S day-1 neutrophils
318 phagocytosis of Zymosan Beads (Mean±SD=28.12±8.39%) was not as effective as that of HD
319 (Mean±SD=50.43±13.04, p=0.02) (Fig.7A). This sepsis-associated decrease of phagocytosis goes with
320 the proportion increase of both CD123+ and PD-L1+ immature neutrophil subsets in the blood of the
321 tested sepsis patients when compared to HD (Fig.7B). t-SNE visualization of PC and NC neutrophils of
322 both *S. aureus* (Fig.7C, D) and Zymosan (Fig.7E, F) bead stimulations highlighted the lower expression
323 level of CD11b marker by S day-1 neutrophils when compared to HD and the default of activation of
324 these cells after microbial beads activation. In fact, S neutrophils exhibited a lower ratio of CD11b and

CD66b MFI between PC and NC after activation, when compared to healthy donors after *S. aureus* (Fig.7D) or Zymosan (Fig.7F) stimulations. The impaired phagocytic capacity of sepsis-patients' immature neutrophils compared to HD neutrophils was confirmed by the measurement of phagocytosed beads MFI ratios between PC and NC. This ratio was three times lower for S day-1 *S. aureus* response (Fig.7D) and 30% lower for S day-1 Zymosan response (Fig.7F). These data allowed the identification of an impaired capacity of immature sepsis neutrophils to form efficient phagolysosomes after bio-particles stimulation and a default of activation when compared to HD.

Discussion

Whole blood mass cytometry and computational analysis identified classical hallmarks of sepsis, and revealed two novel neutrophil subsets that distinguish early sepsis from aseptic inflammatory syndromes. Two novel neutrophil subsets were identified, $CD10^{-}CD64^{+}PD\text{-}L1^{+}$ neutrophils and $CD10^{-}CD64^{+}CD16^{low/-}CD123^{+}$ immature neutrophils that could be used for early identification of sepsis patients. CD123+ and PDL1+ neutrophil subsets could help improving sepsis diagnosis and guide sepsis treatment monitoring.

The results of this study recapitulated previous original findings and meta-analysis studies regarding the sepsis-related increase of circulating immature $CD10^{-}CD64^{+}$ neutrophils (13, 14, 18, 37). Despite all these large efforts, the CD64 detection-based tools are not yet standardized for sepsis diagnosis, because of the heterogeneity of sepsis syndrome and inter-individual variability of CD64 basal level among sepsis patients.

The $CD10^{-}CD64^{+}CD16^{low/-}CD123^{+}$ population is most consistent with immature neutrophils. The frequency of this population among total neutrophils positively correlates with both SAPS II and SOFA

severity scores, and need to be confirmed in a larger collection. The neutrophils expression of CD123 was not described before during sepsis. In a previous study of Weber *et al.,* using a mouse model of abdominal sepsis, the cytokine IL-3 was reported to potentiate inflammation in sepsis by inducing myelopoiesis of neutrophils and IL-3 deficiency protects mice against sepsis (20). Moreover, the authors described an association between high plasma IL-3 levels and high mortality. This result was also obtained in a recent prospective cohort study, where higher levels of IL-3 were shown to be independently associated with hospital mortality in septic patients (21). All these results identify IL-3 and its receptor CD123 as an orchestrator of emergency myelopoiesis, and reveals a new target for the diagnosis and treatment of sepsis.

To our knowledge, the expression of PD-L1 by neutrophil during sepsis was not reported before. It was defined on monocytes, macrophages and endothelial cells (38) but not granulocytes. Monocyte PD-L1 expression was described as an independent predictor of 28-day mortality in patients with septic shock (22, 23). Peripheral blood transcriptomic analysis done by Uhle *et al*., revealed the expression of PD-L1-gene among the top 44 immune-related genes differentially expressed between patients with sepsis and healthy donors (15). In parallel, mice in which the PD-1/PD-L1 interaction was inhibited show improved survival to sepsis (39). Our results bring up a new target for the immune checkpoint therapies.

Controversial results were previously described regarding functional aspects of neutrophils during sepsis. On one hand, Demaret *et al*., described conserved phagocytosis and activation capacities of sepsis neutrophils characterized as $CD10^{dim}CD16^{dim}$ immature cells, after whole blood IL8, fMLP or FITC-labeled *Escherichia coli* stimulation cells (40). On the other hand, Drifte *et al*., by comparing mature and immature neutrophils functions found that the latter were less efficient in phagocytosis and killing. Accordingly, we observed an impaired capacity of cells to form efficient phagolysosomes after bio-particles stimulation and a default of activation when compared to HD.

The immunosuppressive function was also attributed to G-MDSC neutrophils subset during sepsis (13-15, 18). But, to date, human G-MDSC definition lacks consensual phenotypic characterization. Published results on G-MDSC in cancer were obtained according to various phenotypes. Condamine *et al.* described them as Lectin-type oxidized LDL receptor-1 (LOX1) expressing cells (41). Using flow cytometry, we measured the expression of LOX-1 in sepsis patients (data not shown). No LOX-1 co-staining was observed with neither $CD123^+$ nor $PD\text{-}L1^+$ subsets. More investigation is needed to characterize if $CD123^+$ neutrophils and $PD\text{-}L1^+$ subset belong to G-MDSC.

Further research should be conducted to identify appropriate clinical actions for each identified neutrophil subset and their evolution over time course and in different cohorts of patients (undifferentiated shock patients, immunosuppressed patients, different types of infections, durability of neutrophil population after antibiotics), to understand whether altered neutrophil production is responsible for increased sepsis risk, and to determine how these subsets can be therapeutically targeted.

In this study we show that the use of the identified neutrophil subsets gives complementary information to severity scores such as SOFA and SAPS II and are specific of sepsis. In the discovery cohort, in which stringent selection was applied for sepsis and non-infected control patient inclusion, few differences were observed between AUROC of CD123+ neutrophils, SOFA and SAPS II scores (Fig. 4D, F, G). In contrast, the validation cohort, where blind analysis was performed, SOFA and SAPS II lose their discrimination power (Fig. 6D, E) and CD123+ neutrophils biomarker remain highly specific and sensitive for sepsis patient identification.

In addition, the diagnosis of sepsis was evoked for a significant proportion of patients (6/18) in the ICU control group of the validation cohort, a third of them received antibiotics due to their clinical

characteristics but the diagnosis of sepsis was finally dropped out. They ended to be non-infected and undistinguishable from other inflamed and non-infected controls (Supp.Tab.5). Of note, the CD123+ neutrophils proportion of these patients was <0.3%, below the cutoff value identified in our ROC analysis. The use of this biomarker candidate would have avoided this unnecessary administration of antibiotics. Especially that flow cytometry is a widely available technique in the clinic, with reasonable costs and results can be rapidly obtained.

The use of a whole blood flow cytometry test to diagnose sepsis could change the fate of patient's care. The clinician would have a rapid and specific result, obtained before microbiological cultures results, that could guide their therapeutic decision.

In parallel, future studies should now be undertaken to validate the use of these new neutrophil subsets in clinic by routine flow cytometry as an early biomarker predictive of sepsis. Larger cohorts that better represent not only sepsis patients but also the diversity of aseptic inflammatory syndromes need to be evaluated.

Delay to sepsis diagnosis has been shown to decrease survival and increase hospital costs, a better diagnosis will definitely help to improve patient's care, avoid unnecessary treatments and reduce hospital length of stay.

Acknowledgments:

We thank Drs Nicolas Mongardon, Adrien Bouglé, Alice Blet, Pierre Mora, Nicolas Deye and Paul Delval from Assistance-Publique Hôpitaux de Paris, Paris, France, and Dr Delphine Sauce from Cimi-Paris for their help in samples collection.

Conflict of Interest Disclosures:

J.M.I. is a co-founder and a board member of Cytobank Inc. and received research support from Incyte Corp, Janssen, and Pharmacyclics.

Funding:

This work was supported by grants from Inserm, Sorbonne University, Fondation pour la recherche Médicale "Equipe labelisée" and from "Agence Nationale de la Recherche", project CMOS (CX3CR1 expression on monocytes during sepsis) 2015 (ANR-EMMA-050). AMK was supported by post-doctoral fellowship both from the ANR and FRM.

References

1. Seymour CW, Liu VX, Iwashyna TJ, Brunkhorst FM, Rea TD, Scherag A, Rubenfeld G, Kahn JM, Shankar-Hari M, Singer M, Deutschman CS, Escobar GJ, Angus DC. Assessment of Clinical Criteria for Sepsis: For the Third International Consensus Definitions for Sepsis and Septic Shock (Sepsis-3). *Jama* 2016; 315: 762-774.
2. Fleischmann C, Scherag A, Adhikari NK, Hartog CS, Tsaganos T, Schlattmann P, Angus DC, Reinhart K. Assessment of Global Incidence and Mortality of Hospital-treated Sepsis. Current Estimates and Limitations. *American journal of respiratory and critical care medicine* 2016; 193: 259-272.
3. Hotchkiss RS, Moldawer LL, Opal SM, Reinhart K, Turnbull IR, Vincent JL. Sepsis and septic shock. *Nature reviews Disease primers* 2016; 2: 16045.
4. Yang Y, Xie J, Guo F, Longhini F, Gao Z, Huang Y, Qiu H. Combination of C-reactive protein, procalcitonin and sepsis-related organ failure score for the diagnosis of sepsis in critical patients. *Annals of intensive care* 2016; 6: 51.
5. Moreno R, Vincent JL, Matos R, Mendonça A, Cantraine F, Thijs L, Takala J, Sprung C, Antonelli M, Bruining H, Willatts S. The use of maximum SOFA score to quantify organ dysfunction/failure in intensive care. Results of a prospective, multicentre study. Working

Group on Sepsis related Problems of the ESICM. *Intensive care medicine* 1999; 25: 686-696.

6. Wasserman A, Karov R, Shenhar-Tsarfaty S, Paran Y, Zeltzer D, Shapira I, Trotzky D, Halpern P, Meilik A, Raykhshtat E, Goldiner I, Berliner S, Rogowski O. Septic patients presenting with apparently normal C-reactive protein: A point of caution for the ER physician. *Medicine (Baltimore)* 2019; 98: e13989.
7. Minne L, Abu-Hanna A, de Jonge E. Evaluation of SOFA-based models for predicting mortality in the ICU: A systematic review. *Critical care (London, England)* 2008; 12: R161.
8. Singer M, Deutschman CS, Seymour CW, Shankar-Hari M, Annane D, Bauer M, Bellomo R, Bernard GR, Chiche JD, Coopersmith CM, Hotchkiss RS, Levy MM, Marshall JC, Martin GS, Opal SM, Rubenfeld GD, van der Poll T, Vincent JL, Angus DC. The Third International Consensus Definitions for Sepsis and Septic Shock (Sepsis-3). *Jama* 2016; 315: 801-810.
9. Kumar A, Roberts D, Wood KE, Light B, Parrillo JE, Sharma S, Suppes R, Feinstein D, Zanotti S, Taiberg L, Gurka D, Kumar A, Cheang M. Duration of hypotension before initiation of effective antimicrobial therapy is the critical determinant of survival in human septic shock. *Critical care medicine* 2006; 34: 1589-1596.
10. van der Poll T, van de Veerdonk FL, Scicluna BP, Netea MG. The immunopathology of sepsis and potential therapeutic targets. *Nature reviews Immunology* 2017; 17: 407-420.
11. Treacher DF, Sabbato M, Brown KA, Gant V. The effects of leucodepletion in patients who develop the systemic inflammatory response syndrome following cardiopulmonary bypass. *Perfusion* 2001; 16 Suppl: 67-73.
12. Brown KA, Brain SD, Pearson JD, Edgeworth JD, Lewis SM, Treacher DF. Neutrophils in development of multiple organ failure in sepsis. *Lancet (London, England)* 2006; 368: 157-169.
13. Daix T, Guerin E, Tavernier E, Mercier E, Gissot V, Herault O, Mira JP, Dumas F, Chapuis N, Guitton C, Bene MC, Quenot JP, Tissier C, Guy J, Piton G, Roggy A, Muller G, Legac E, de Prost N, Khellaf M, Wagner-Ballon O, Coudroy R, Dindinaud E, Uhel F, Roussel M, Lafon T, Jeannet R, Vargas F, Fleureau C, Roux M, Allou K, Vignon P, Feuillard J,

Francois B. Multicentric Standardized Flow Cytometry Routine Assessment of Patients With Sepsis to Predict Clinical Worsening. *Chest* 2018; 154: 617-627.

14. Guerin E, Orabona M, Raquil MA, Giraudeau B, Bellier R, Gibot S, Bene MC, Lacombe F, Droin N, Solary E, Vignon P, Feuillard J, Francois B. Circulating immature granulocytes with T-cell killing functions predict sepsis deterioration*. *Critical care medicine* 2014; 42: 2007-2018.
15. Uhel F, Azzaoui I, Gregoire M, Pangault C, Dulong J, Tadie JM, Gacouin A, Camus C, Cynober L, Fest T, Le Tulzo Y, Roussel M, Tarte K. Early Expansion of Circulating Granulocytic Myeloid-derived Suppressor Cells Predicts Development of Nosocomial Infections in Patients with Sepsis. *American journal of respiratory and critical care medicine* 2017; 196: 315-327.
16. Mahmoodpoor A, Paknezhad S, Shadvar K, Hamishehkar H, Movassaghpour AA, Sanaie S, Ghamari AA, Soleimanpour H. Flow Cytometry of CD64, HLA-DR, CD25, and TLRs for Diagnosis and Prognosis of Sepsis in Critically Ill Patients Admitted to the Intensive Care Unit: A Review Article. *Anesthesiology and pain medicine* 2018; 8: e83128.
17. Barth E, Fischer G, Schneider EM, Wollmeyer J, Georgieff M, Weiss M. Differences in the expression of CD64 and mCD14 on polymorphonuclear cells and on monocytes in patients with septic shock. *Cytokine* 2001; 14: 299-302.
18. Bae MH, Park SH, Park CJ, Cho EJ, Lee BR, Kim YJ, Park SH, Cho YU, Jang S, Song DK, Hong SB. Flow cytometric measurement of respiratory burst activity and surface expression of neutrophils for septic patient prognosis. *Cytometry Part B, Clinical cytometry* 2016; 90: 368-375.
19. Elghetany MT. Surface antigen changes during normal neutrophilic development: a critical review. *Blood cells, molecules & diseases* 2002; 28: 260-274.
20. Weber GF, Chousterman BG, He S, Fenn AM, Nairz M, Anzai A, Brenner T, Uhle F, Iwamoto Y, Robbins CS, Noiret L, Maier SL, Zonnchen T, Rahbari NN, Scholch S, Klotzsche-von Ameln A, Chavakis T, Weitz J, Hofer S, Weigand MA, Nahrendorf M, Weissleder R, Swirski FK. Interleukin-3 amplifies acute inflammation and is a potential therapeutic target in sepsis. *Science (New York, NY)* 2015; 347: 1260-1265.

21. Borges IN, Resende CB, Vieira ELM, Silva J, Andrade MVM, Souza AJ, Badaro E, Carneiro RM, Teixeira AL, Jr., Nobre V. Role of interleukin-3 as a prognostic marker in septic patients. *Revista Brasileira de terapia intensiva* 2018; 30: 443-452.
22. Shao R, Fang Y, Yu H, Zhao L, Jiang Z, Li CS. Monocyte programmed death ligand-1 expression after 3-4 days of sepsis is associated with risk stratification and mortality in septic patients: a prospective cohort study. *Critical care (London, England)* 2016; 20: 124.
23. Tai H, Xing H, Xiang D, Zhu Z, Mei H, Sun W, Zhang W. Monocyte Programmed Death Ligand-1, A Predicator for 28-Day Mortality in Septic Patients. *The American journal of the medical sciences* 2018; 355: 362-367.
24. Bendall SC, Simonds EF, Qiu P, Amir el AD, Krutzik PO, Finck R, Bruggner RV, Melamed R, Trejo A, Ornatsky OI, Balderas RS, Plevritis SK, Sachs K, Pe'er D, Tanner SD, Nolan GP. Single-cell mass cytometry of differential immune and drug responses across a human hematopoietic continuum. *Science (New York, NY)* 2011; 332: 687-696.
25. Greenplate AR, Johnson DB, Ferrell PB, Jr., Irish JM. Systems immune monitoring in cancer therapy. *European journal of cancer* 2016; 61: 77-84.
26. Irish JM. Beyond the age of cellular discovery. *Nature immunology* 2014; 15: 1095-1097.
27. Finck R, Simonds EF, Jager A, Krishnaswamy S, Sachs K, Fantl W, Pe'er D, Nolan GP, Bendall SC. Normalization of mass cytometry data with bead standards. *Cytometry Part A : the journal of the International Society for Analytical Cytology* 2013; 83: 483-494.
28. Kotecha N, Krutzik PO, Irish JM. Web-based analysis and publication of flow cytometry experiments. *Current protocols in cytometry* 2010; Chapter 10: Unit10.17.
29. Amir el AD, Davis KL, Tadmor MD, Simonds EF, Levine JH, Bendall SC, Shenfeld DK, Krishnaswamy S, Nolan GP, Pe'er D. viSNE enables visualization of high dimensional single-cell data and reveals phenotypic heterogeneity of leukemia. *Nature biotechnology* 2013; 31: 545-552.
30. Becht E, McInnes L, Healy J, Dutertre CA, Kwok IWH, Ng LG, Ginhoux F, Newell EW. Dimensionality reduction for visualizing single-cell data using UMAP. *Nature biotechnology* 2018.

31. Qiu P, Simonds EF, Bendall SC, Gibbs KD, Jr., Bruggner RV, Linderman MD, Sachs K, Nolan GP, Plevritis SK. Extracting a cellular hierarchy from high-dimensional cytometry data with SPADE. *Nature biotechnology* 2011; 29: 886-891.
32. Van Gassen S, Callebaut B, Van Helden MJ, Lambrecht BN, Demeester P, Dhaene T, Saeys Y. FlowSOM: Using self-organizing maps for visualization and interpretation of cytometry data. *Cytometry Part A : the journal of the International Society for Analytical Cytology* 2015; 87: 636-645.
33. Leelatian N, Sinnaeve J, Mistry AM, Barone SM, Diggins KE, Greenplate AR, Weaver KD, Thompson RC, Chambless LB, Mobley BC, Ihrie RA, Irish JM. High risk glioblastoma cells revealed by machine learning and single cell signaling profiles. *bioRxiv* 2019: 632208.
34. Diggins KE, Gandelman JS, Roe CE, Irish JM. Generating Quantitative Cell Identity Labels with Marker Enrichment Modeling (MEM). *Current protocols in cytometry* 2018; 83: 10.21.11-10.21.28.
35. Diggins KE, Greenplate AR, Leelatian N, Wogsland CE, Irish JM. Characterizing cell subsets using marker enrichment modeling. *Nature methods* 2017; 14: 275-278.
36. Neaga A, Lefor J, Lich KE, Liparoto SF, Xiao YQ. Development and validation of a flow cytometric method to evaluate phagocytosis of pHrodo BioParticles(R) by granulocytes in multiple species. *Journal of immunological methods* 2013; 390: 9-17.
37. Wang X, Li ZY, Zeng L, Zhang AQ, Pan W, Gu W, Jiang JX. Neutrophil CD64 expression as a diagnostic marker for sepsis in adult patients: a meta-analysis. *Critical care (London, England)* 2015; 19: 245.
38. Boomer JS, To K, Chang KC, Takasu O, Osborne DF, Walton AH, Bricker TL, Jarman SD, 2nd, Kreisel D, Krupnick AS, Srivastava A, Swanson PE, Green JM, Hotchkiss RS. Immunosuppression in patients who die of sepsis and multiple organ failure. *Jama* 2011; 306: 2594-2605.
39. Huang X, Venet F, Wang YL, Lepape A, Yuan Z, Chen Y, Swan R, Kherouf H, Monneret G, Chung CS, Ayala A. PD-1 expression by macrophages plays a pathologic role in altering microbial clearance and the innate inflammatory response to sepsis. *Proceedings of the National Academy of Sciences of the United States of America* 2009; 106: 6303-6308.

40. Demaret J, Venet F, Friggeri A, Cazalis MA, Plassais J, Jallades L, Malcus C, Poitevin-Later F, Textoris J, Lepape A, Monneret G. Marked alterations of neutrophil functions during sepsis-induced immunosuppression. *Journal of leukocyte biology* 2015; 98: 1081-1090.

41. Condamine T, Dominguez GA, Youn JI, Kossenkov AV, Mony S, Alicea-Torres K, Tcyganov E, Hashimoto A, Nefedova Y, Lin C, Partlova S, Garfall A, Vogl DT, Xu X, Knight SC, Malietzis G, Lee GH, Eruslanov E, Albelda SM, Wang X, Mehta JL, Bewtra M, Rustgi A, Hockstein N, Witt R, Masters G, Nam B, Smirnov D, Sepulveda MA, Gabrilovich DI. Lectin-type oxidized LDL receptor-1 distinguishes population of human polymorphonuclear myeloid-derived suppressor cells in cancer patients. *Science immunology* 2016; 1.

Figure Legends:

Fig.1. Study design. (**A**) Blood samples from sepsis patients (S) (n=17) or non-infected post-cardiothoracic surgery patients (NIC) (n=12) were enrolled in the discovery cohort of the study, in addition, blood samples were obtained from healthy donors (HD) (n=11) and bone marrows biopsies from orthopedic surgery patients (BM) (n=5). Immunostainings targeting 42 parameters were performed and analyzed by mass cytometry. A computational "discovery strategy" was used to identify sepsis-specific subsets (**B**), a "computational validation" analysis was used to check whether the identified sepsis-specific subsets are strategy-dependant (**C**), and with an additional "expert driven validation" we defined a small set of markers to gate on the sepsis-specific neutrophil subsets (**D**). A second independent validation cohort, with sepsis patients (S) (n=24) and noninfected patients (NIP) (n=18), was used for the "biological validation" of these sepsis-specific neutrophil subsets by conventional flow cytometry (**E**).

Fig.2. Identification of sepsis day 1-specific neutrophils with a discovery analysis strategy. (A) t-SNE analysis was performed on neutrophils from all samples with cells being organized along t-SNE-1-2

583 and t-SNE-2-2 according to per-cell expression of CD11b, CD66b, CD16, CD10, CD64 and CD123,
584 PD-L1. Cell density for the concatenated file of each group is shown, on a black to yellow heat scale,
585 for each group time-point. (**B**) A heat map shows samples clustering (columns) according to nodes
586 cell proportion log2-transformed and centered around the mean proportion of all samples' nodes
587 (rows). Samples and mean-centered log2-transformed nodes cell proportion were arranged according
588 to complete linkage hierarchical clustering. Heat intensity (from blue to yellow) reflects the mean-
589 centered log2-transformed cell proportion of each sample's node. (**C**) A heatmap shows
590 characterization of cell nodes identified by SPADE (columns) according to mean expression of 7
591 markers (rows). Markers were arranged according to complete linkage hierarchical clustering and
592 nodes were pre-ordered according to (**B**) heat map nodes order. Heat intensity (from blue to red)
593 reflects the mean expression of each marker for each node. (**D**) Four groups of nodes were back-
594 viewed on t-SNE1-2 / t-SNE2-2 map. (**E**) cells abundance of each meta-cluster subset (CD10-
595 CD64+CD16+PD-L1+ cell subset in red, CD10-CD64+CD16lowCD123+ cell subset in blue and
596 CD10-CD64+ cell subset in green) was presented as cell proportion among total neutrophils of each
597 group samples. Statistics: Nonparametric two-tailed Mann-Whitney test was used to compare
598 differences in cellular abundance of cell subsets between NIC-D1 and S-D1 (see the Methods
599 section). Sample sizes: HD=11, BM=5, NIC=12 and S=17.

600 **Fig.3. Validation of sepsis day-1-specific neutrophil subsets by a second computational strategy.** As
601 a first step, UMAP analysis was performed on all samples neutrophils and cells were organized along
602 UMAP-1 and UMAP-2 axes according to per-cell expression of CD11b, CD66b, CD16, CD10, CD64
603 and CD123, PD-L1. As a second step, FlowSOM clustering was done to separate neutrophils subsets
604 into 50 clusters. MEM was then used to quantify the enriched features of the 50 clusters. Protein
605 enrichment was reported on a +10 to −10 scale, where +10 indicates that protein's expression was

especially enriched and −10 indicated that the protein's expression was excluded from those cells, relative to the other neutrophils clusters. (**A**) Among these clusters, two meta-clusters were identified as phenotypically identical to the strategy-1 sepsis-specific neutrophils: clusters 18 and 19 (in red) composed of CD10-CD64+PD-L1+ neutrophils and clusters 6 and 7 (in blue) composed of CD10-CD64+ CD16lowCD123+ neutrophils. (**B**) Cells abundance of each meta-cluster subset (CD10-CD64+CD16+PD-L1+ cell subset in red and CD10-CD64+CD16lowCD123+ cell subset in blue) was presented as cell proportion among total neutrophils of each group samples. Statistics: Nonparametric two-tailed Mann-Whitney test was used to compare differences in cellular abundance of cell subsets between NIC-D1 and S-D1 (see the Methods section). Sample sizes: HD=11, BM=5, NIC=12 and S=17. (**C**) each meta-cluster cells (red and blue) was back-viewed on both UMAP-1 / UMAP-2 map, and t-SNE1-2 / t-SNE2-2 map.

Fig.4. Sepsis day 1-specific neutrophil subsets validated by expert gating correlate with severity scores. Expert gating strategy with 7 markers set (**A**) allowed the selection of CD10-CD64+PD-L1+ cell subset (in red) and CD10-CD64+CD16lowCD123+ cell subset (in blue), back-viewed on both discovery (t-SNE1-2 / t-SNE2-2) and validation (UMAP-1 / UMAP-2) maps. The two neutrophil subsets are significantly more abundant in sepsis patients (S) blood collected at day-1 post-admission to ICU when compared to day-1 or day-7 non-infected post-cardiothoracic surgery patients (NIC) or Healthy donors (HD) (**B**). Correlation between the log10 transformed frequency of $CD10^{-}CD64^{+}PD\text{-}L1^{+}$ neutrophils subset (in red) or $CD10^{-}CD64^{+}CD16^{low}CD123^{+}$ neutrophils subset (in blue) and SAPS II score (green squares) or SOFA score (purple squares) are shown in (**C**). ROC curve obtained using only $CD123^{+}$ neutrophil subset is shown in (**D**) and the one using $CD123^{+}PD\text{-}L1^{+}$ neutrophil subsets is shown in **(E)** and with the SOFA and SAPS II clinical scores are shown in **(F)** and **(G)** respectively. Statistics: Nonparametric two-tailed Mann-Whitney test was used to compare cellular

abundances of cell subsets between S-D1 and NIC-D1, NIC-D7 or HD. Nonparametric two-tailed Wilcoxon signed-rank test was used to compare cellular abundances between the two matched groups S-D1 and S-D7. Linear regression lines and Spearman's rank correlation were used to assess relationship between neutrophil subsets frequency and severity scores (see the Methods section). Spearman r and tow-tailed *p* value are presented. * $p<0.05$. Sample sizes: HD=11, BM=5, NIC=12 and S=17.

Fig.5. Non-neutrophil cells analysis resume sepsis immune hallmarks. (A) Lymphocytes and monocytes numbers and intensity of HLA-DR expression on monocytes (mHLA-DR) were obtained from non-neutrophils computational analysis and presented for each group. **(B)** Neutrophils numbers were obtained previously from the computational separation of neutrophils from non-neutrophil cells and used to calculate Neutrophils/Lymphocytes ratio. Cell number of the main immune subsets that were differentially abundant in S group from HD and NIC were presented in **(C)** and the ones that were differentially abundant in S group from only HD were presented in **(D)**.

Fig.6. Sepsis-specific neutrophils are detectable by conventional cytometry and discriminate infected from non-infected patients. The gating strategy applied on fluorescent flow cytometry data of three sepsis patients from the validation cohort is showed in (**A**). The overlay of full minus-two (FMT) stained control and the full panel (FP) stained tubes of each representative patient, showed the increase of sepsis-specific neutrophil subsets with the decrease of CD10 expression by neutrophils (CD14-CRTH2-CD15+ cells). The ROC curves were obtained using only $CD123^+$ neutrophil subset (**B**), the two $CD123^+$ and PD-$L1^+$ neutrophil subsets **(C)** or using the SOFA **(D)** and SAPS II **(E)** clinical scores.

Fig.7. Staphylococcus aureus and Zymosan specific activation and phagocytosis are impaired in immature sepsis neutrophils. To address sepsis immature (CD64+CD10-) neutrophils phagocytic capacities, 100µL of blood were incubated with 20µL or 40µL of beads coated with Staphylococcus aureus or Zymosan, respectively, coated-particles and coupled with pH acidification-sensitive fluorochrome. After 1h incubation at 37°C (PC: positive control) or 4°C (NC: negative control) cells were stained and analyzed by flow cytometry. (**A**) represents gating strategy of CD15+CD14-CD3-CD19- neutrophils from healthy donors (HD), sepsis day-1 samples (S-D1) and bone marrow samples (BM). Cells were separated in 2 gates based on CD10 expression and phagocytosis marker intensity (Staphylococcus aureus or Zymosan) and cells from PC (red dots) were overlaid on NC cells (blue dots). The proportion of total phagocytic neutrophils were presented for the three groups. t-SNE analysis organized cells along t-SNE axes according to per-cell expression of 5 proteins and phagocytosis fluorescence. Cell expression of CD11b after Staphylococcus aureus (**B**) or Zymosan (**C**) stimulations, for one representative individual of HD and S-D1 stimulated at +4°C (NC) and +37°C (PC) is shown on a heat scale. The ratio between PC and NC CD66b CD11b and particles MFI, of each individual after Staphylococcus aureus (**D**) or Zymosan (**E**) stimulations, in each group were plotted in histograms. CD10- cells have less phagocytic capacity whatever it is appreciated by MFI or proportion. Stimulated CD10- cells exhibit a lower level of expression of CD11b and CD66b. Statistics: Nonparametric two-tailed Mann-Whitney test was used to compare differences in cellular abundance of cell subsets and MFI ratios (see the Methods section). Sample sizes: HD=4, S-D1=6 and BM=3.

Figures:

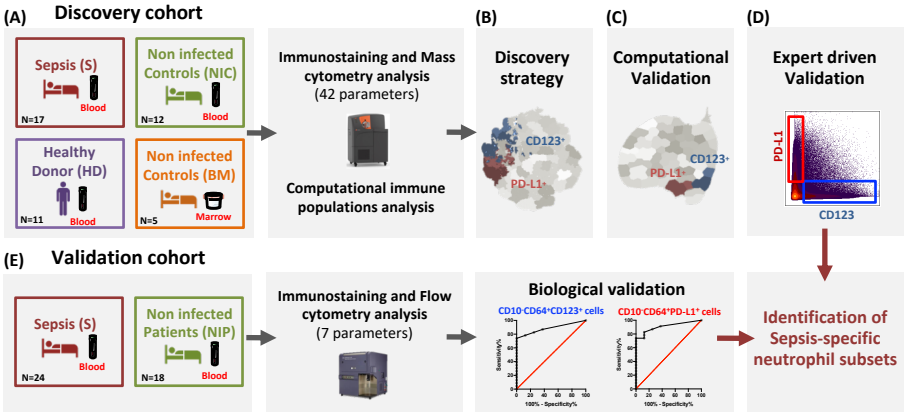

Figure 1. Study design

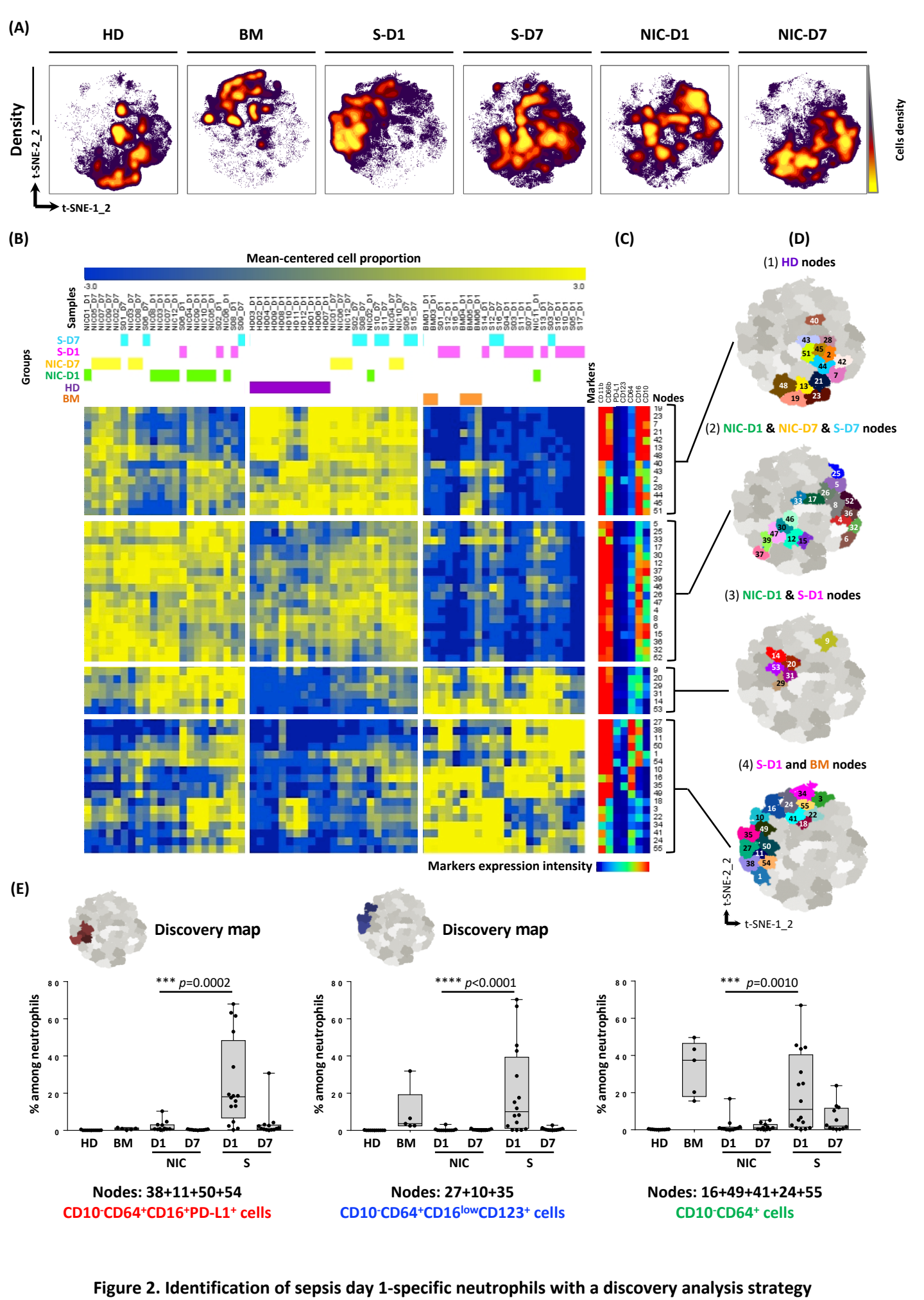

Figure 2. Identification of sepsis day 1-specific neutrophils with a discovery analysis strategy

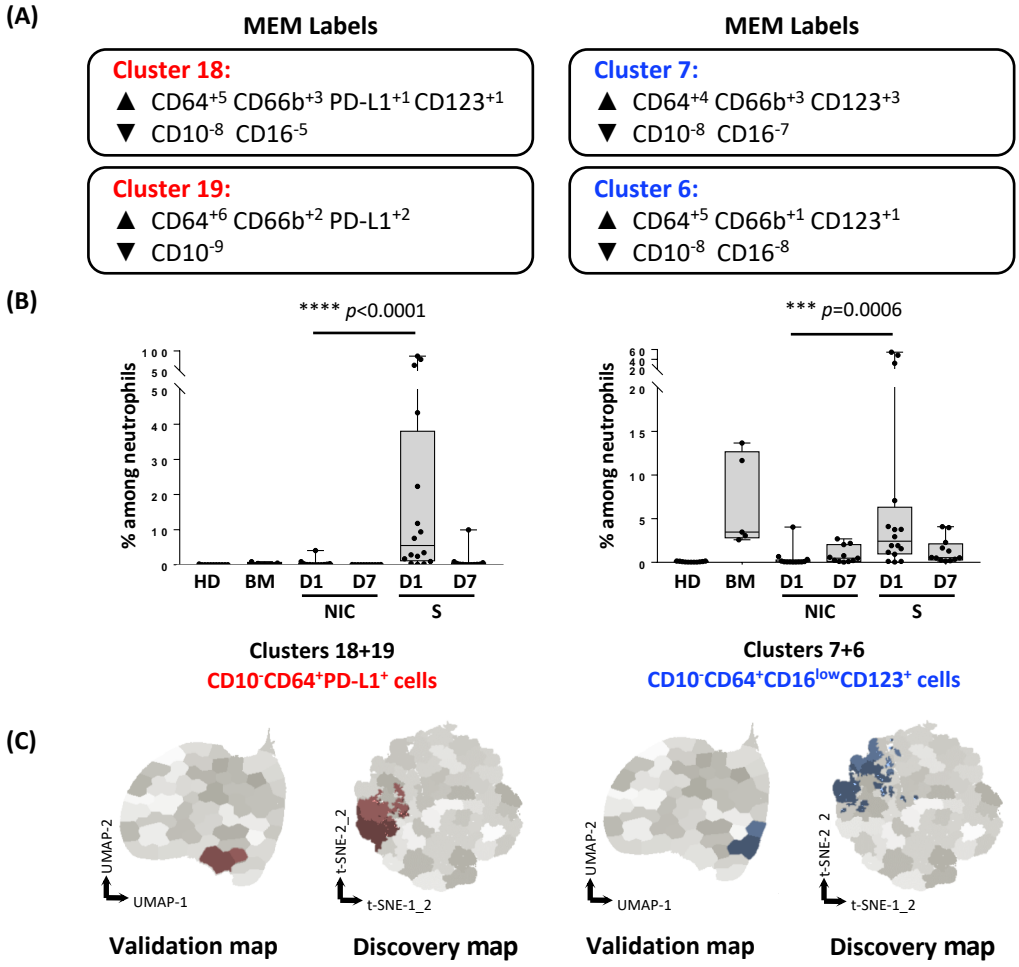

Figure 3. Validation of sepsis day-1-specific neutrophil subsets by a second computational strategy

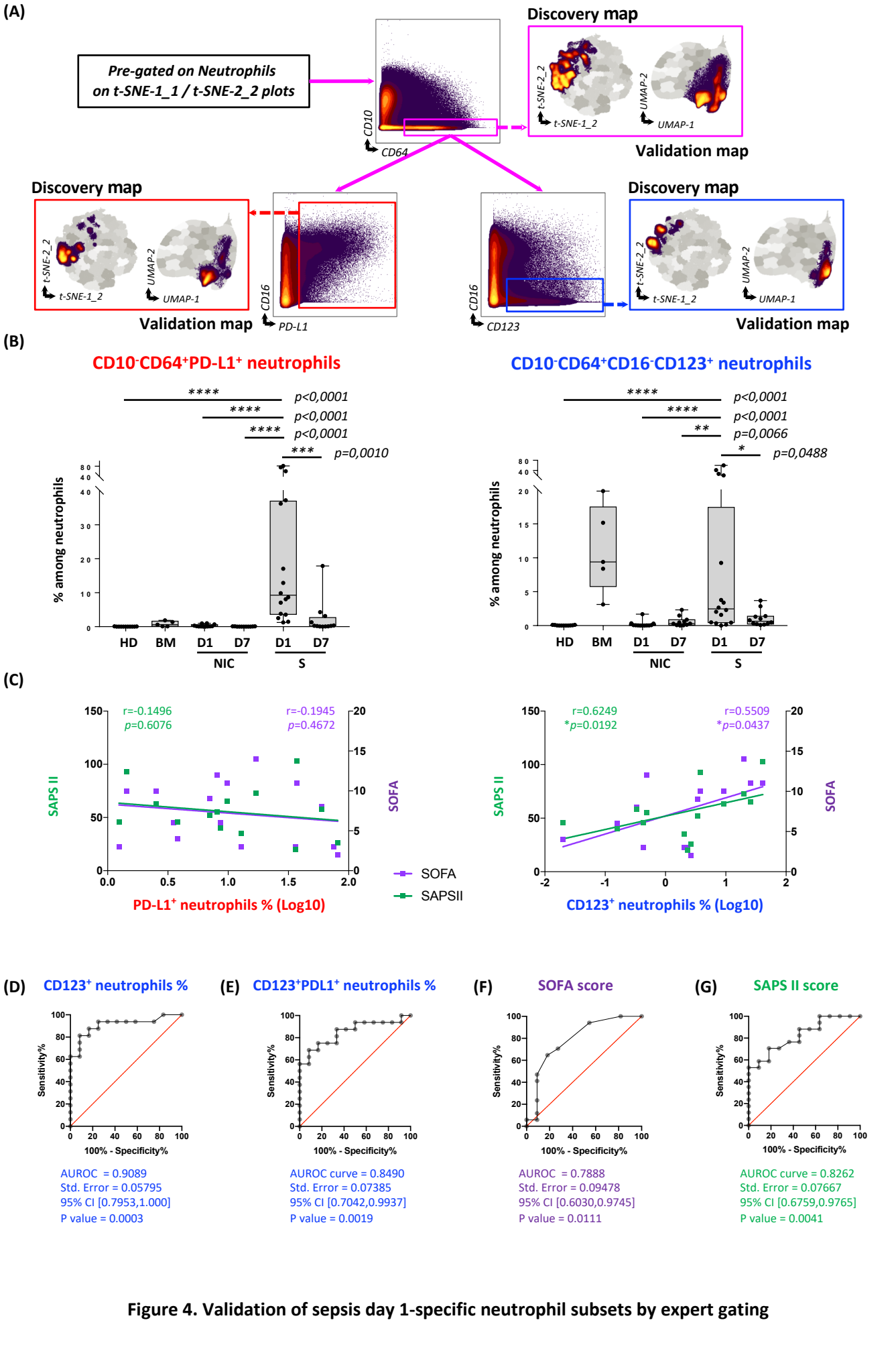

Figure 4. Validation of sepsis day 1-specific neutrophil subsets by expert gating

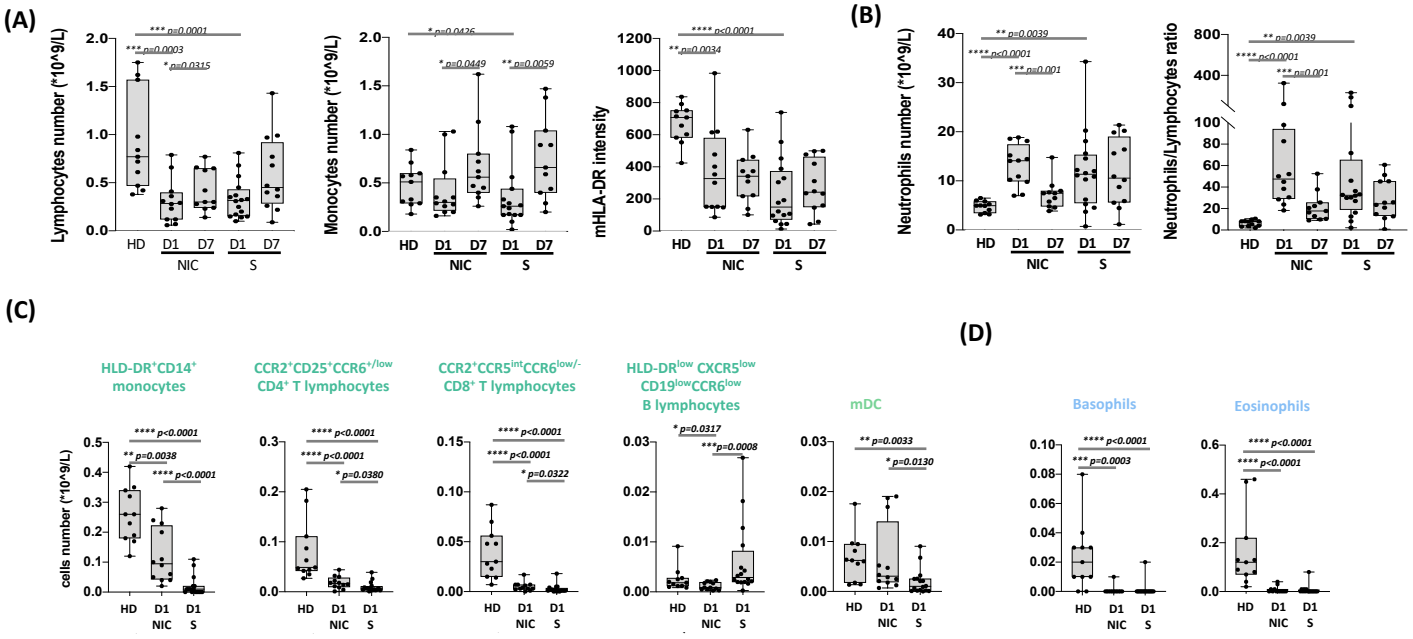

(C)

(D)

Figure 5. Non-neutrophil cells analysis resume sepsis immune hallmarks

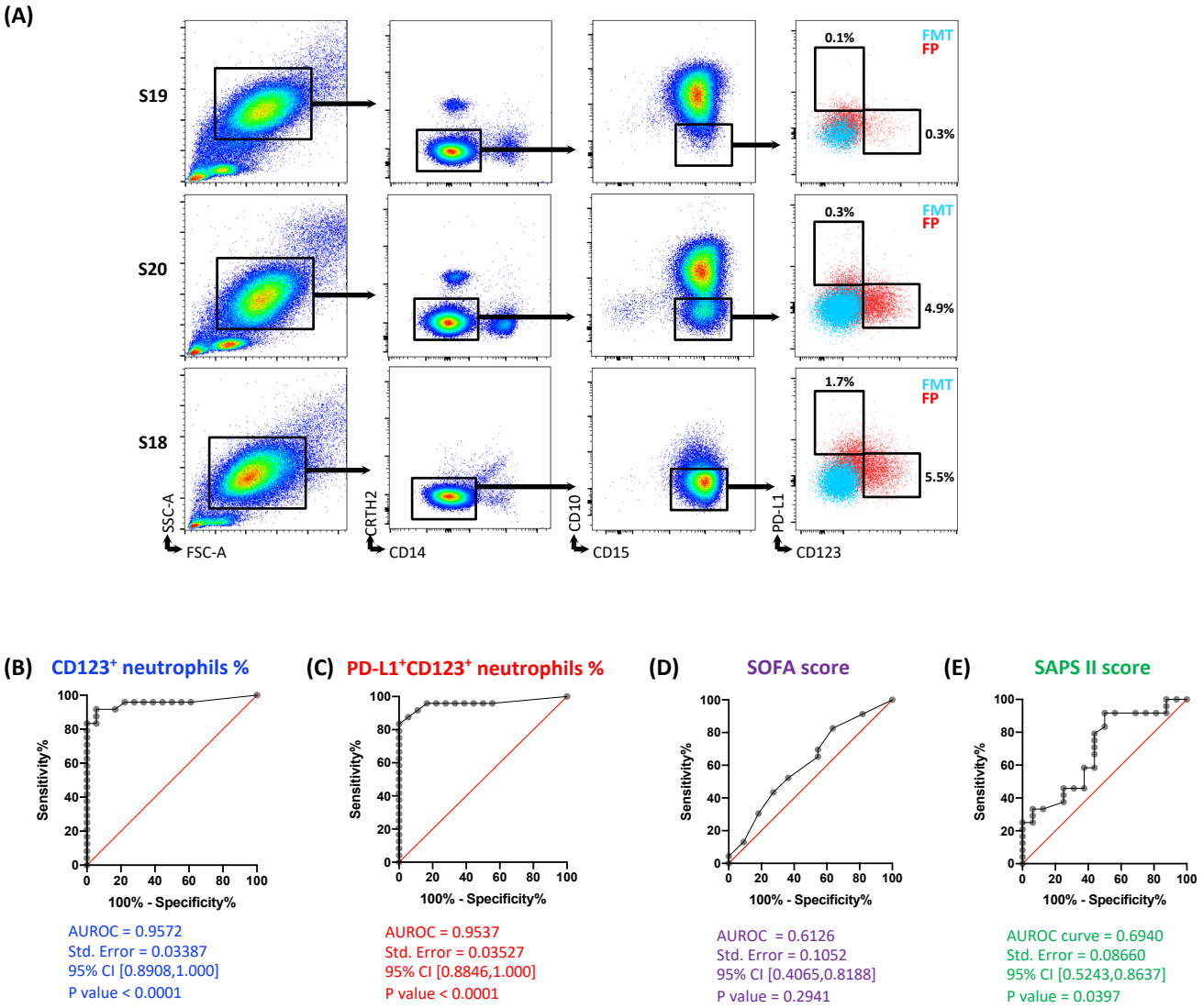

Figure 6. Sepsis-specific neutrophils are detectable by conventional cytometry and discriminate infected from non-infected patients

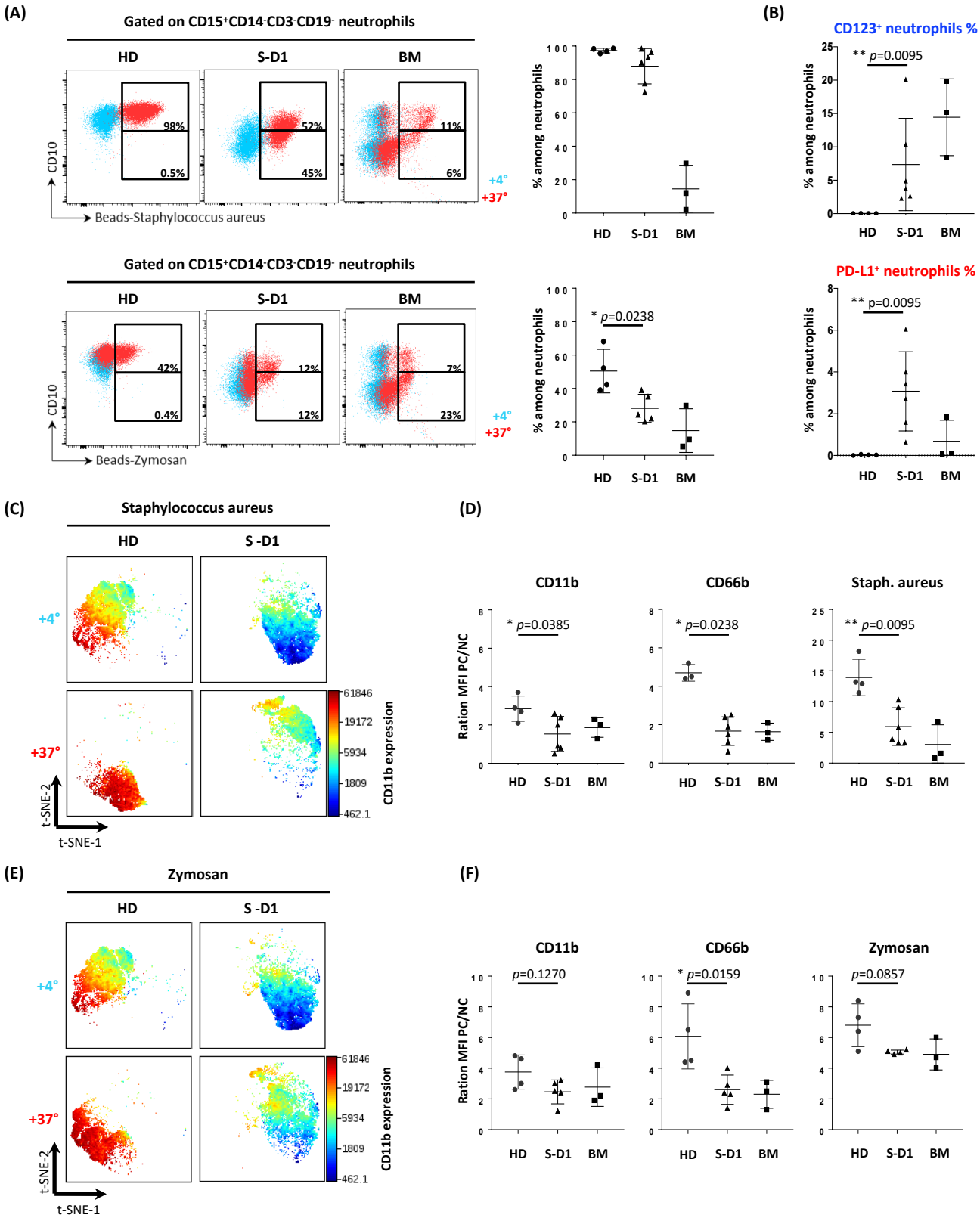

Figure 7. Staphylococcus aureus and Zymosan specific activation and phagocytosis are impaired in immature sepsis neutrophils